Noname manuscript No.
(will be inserted by the editor)

Detumbling a Non-cooperative Target with Unknown Inertial Parameters using a Space Robot Under Control Input Magnitude Constraint

Rabindra Gangapersaud · Guangjun Liu · Anton de Ruiter

Received: date / Accepted: date

Abstract The detumbling of a non-cooperative tumbling target by a space robot is a challenging endeavour. Previous studies have formulated detumbling strategies by making either or both of the following assumptions: (1) the availability of force/torque measurements; (2) accurate knowledge of the target's inertial parameters (mass, inertia tensor, location of center of mass). In reality, the target's inertial parameters are uncertain and force/torque measurements are difficult to obtain due to the harsh environment of space. This study presents a robust adaptive detumbling controller to detumble a non-cooperative target with unknown inertial parameters that lie within known bounds, without the need of force/torque measurements. Furthermore, the proposed detumbling strategy takes into account magnitude limits on the control inputs of the space robot that consists of a manipulator and a satellite. A hyperbolic tangent function is employed to model the magnitude constraints of the space robot's control input, which results in a system that is non-affine in its control inputs. An augmented model of the space robot is formulated to allow the development of the detumbling controller. Using bounds on the target's inertial parameters, robust adaptive control approach is utilized to design the detumbling controller with the backstepping technique to ensure successful detumbling of the unknown target attached to the end-effector and rejection of its momentum. The performance of the proposed robust adaptive detumbling controller is examined through numerical simulations, and its effectiveness in detumbling a non-cooperative target with unknown inertial parameters is demonstrated.

Keywords Space robotic manipulator · Non-cooperative target · Robust control

1 Introduction

The capture and servicing of a malfunctioning satellite, denoted as the target, is a challenging problem as it is common for the target to be non-cooperative, tumbling and for its inertial parameters (mass, inertia tensor and location of center of mass) to be uncertain [4]. The research community has proposed the use of a robotic manipulator attached to a satellite base to capture and the target and is denoted as the servicer. The capture process is typically

R. Gangapersaud*, G. Liu, A. de Ruiter
Department of Aerospace Engineering, Ryerson University, Toronto, Ontario, Canada
*Corresponding author, E-mail: amar.r.gangapersaud@ryerson.ca

segmented into pre-grasping, contact and post-grasping phases. In the pre-grasping and capture phase, the servicer is concerned with rendezvousing with the target's grasping surface and physically grasping the target [3, 4]. After the target is rigidly grasped by the servicer's end-effector in the contact phase, the post-grasping phase is concerned with bringing the target's tumbling motion to rest subjected to interaction force/torque limits at the grasping point [3, 4].

The authors of [2, 3, 5, 17] have achieved detumbling of the target in the post-grasping phase by assuming that the target's inertial parameters are accurately known. Under this assumption, coordination of the servicer's end-effector and base to track a desired detumbling trajectory and reject the target's momentum with the target attached to the end-effector is accomplished. However, it is unrealistic to assume that the target's inertial parameters can be accurately known prior to the post-grasping phase (e.g., no practical way to measure remaining propellant in a malfunctioning satellite).

To address uncertainty in the target's inertial parameters, [18] and [13] have delineated desired detumbling trajectories without requiring accurate knowledge of the target's inertial parameters. However, in [13], there is no consideration of the target's parameter uncertainty in the servicer's controller design to track the desired detumbling trajectory and to accommodate the target's momentum. In [18] and [1], with the use of force/torque measurements at the end-effector, impedance control is utilized to track the desired detumbling trajectory with an uncertain target attached to the end-effector. The requirement of force/torque measurements in [18] and [1] is difficult to satisfy in space due to the operational issues that arise in the space environment [11]. In [22], an adaptive sliding mode controller is presented to track a desired detumbling trajectory with an uncertain target attached to its end-effector. The authors achieve robustness to target parameter uncertainty without the need of end-effector's force/torque measurements.

The above-mentioned detumbling strategies achieve detumbling of the target by tracking a desired detumbling trajectory. However, they do so without consideration of limits of the servicer's control inputs and in some cases requires force/torque measurements at the servicer's end-effector. In practical application, the servicer will be subjected to limits on its control input because of physical limits of the onboard actuators. A tracking controller to track a desired detumbling trajectory must consider these limits in the controller's design as they may lead to instability or poor performance if not considered. This study takes into account magnitude limits on the servicer's control inputs by modelling them with a hyperbolic tangent function, which results in a system that is non-affine in its control inputs. An augment model of the servicer is introduced, and with the use of the backstepping technique and bounds on the target's inertial parameters, a controller to track a desired detumbling trajectory subjected to control input magnitude constraints is presented. The resultant detumbling controller does not require force/torque measurements at the servicer's end-effector.

The remainder of the paper is organized as follows. Section 2 presents the scenario and assumptions along with dynamics and kinematics of the servicer and target. Section 3 presents the development of the robust trajectory tracking controller. Section 4 presents numerical simulations results of the proposed robust trajectory tracking controller. Concluding remarks are given in Section 5.

2 Problem Formulation

The following assumptions are utilized in developing the proposed detumbling controller: (1) measurements of the servicer's base linear and angular velocities are available; (2) the

target is rigidly attached to the end-effector after grasping (firmly grasped); and (3) the relative linear velocity between the center of mass of the servicer and target prior to capture is zero.

The first assumption implies that measurements of the servicer system are available from the inertial frame. This can be made possible if there exists an inertial observer such as a camera on an external space structure as proposed by [14], or a second satellite in formation with the servicer. To realize the last assumption, vehicular operations of the servicer satellite are assumed to have been utilized to guide the servicer to a pose where the relative velocity of the servicer and target are near zero and the servicer's manipulator can reach out and capture the target. Under these conditions, the combined servicer-target system after capture will have zero linear momentum relative to the inertial observer as the problem of absorbing and dissipating the gained linear momentum by the servicer with the use of external jet thruster is not addressed. These assumptions are common in the literature on detumbling of a non-cooperative target [6, 12, 13, 21].

As a result of the above stated assumptions, the following Corollary can be stated:

Corollary 1 *The servicer is composed of multiple rigid bodies that are physically constrained to each other via revolute joints and the target is rigidly attached to the servicer's end-effector (Assumption 2), i.e., the maximum distance between the end-effector and the center of mass of any rigid body of the servicer/target system is geometrically constrained. From Assumption 3, it follows that the end-effector's position is also bounded from an inertial frame of reference located at the center of mass of the combined servicer/target system.*

2.1 Notations

The following notations are used: a right upper superscript d as in $(\cdot)^{\mathrm{d}}$, denotes the desired value of $(\cdot)$; $\mathbf{E}_n \in \mathbb{R}^{n\times n}$ is an identity matrix; $\lambda_{\max}(\cdot)$ and $\lambda_{\min}(\cdot)$ denote the maximum and minimum eigenvalues of symmetric matrix $(\cdot)$, respectively; for the vector $\mathbf{x} \in \mathbb{R}^3$, the skew-symmetric matrix is denoted as $\mathbf{x}^\times$ such that $\mathbf{x}^\times \mathbf{a} = \mathbf{x} \times \mathbf{a}$ for any $\mathbf{a} \in \mathbb{R}^3$.

2.2 Servicer-Target Dynamics

The space robot consists of a base body and m-link serial manipulator arm. Let $\boldsymbol{\nu}_{\mathrm{b}} = [\mathbf{v}_{\mathrm{b}}^{\mathrm{T}}, \mathbf{w}_{\mathrm{b}}^{\mathrm{T}}]^{\mathrm{T}} \in \mathbb{R}^6$ and $\boldsymbol{\nu}_{\mathrm{e}} = [\mathbf{v}_{\mathrm{e}}^{\mathrm{T}}, \mathbf{w}_{\mathrm{e}}^{\mathrm{T}}]^{\mathrm{T}} \in \mathbb{R}^6$ represent the linear and angular velocity of the servicer's base center of mass and the end-effector's linear and angular velocity, respectively. Making use of the expression for linear and angular momentum of the servicer and the kinematic relationship between the servicer's end-effector, base and manipulator velocities, one can arrive at the following equation of motion for the servicer as in [7, 8]:

$$\mathbf{M}_{\mathrm{s}}\dot{\boldsymbol{\xi}} + \mathbf{c}_{\mathrm{s}} = \mathbf{A}^{\mathrm{T}}\boldsymbol{\tau} + \mathbf{J}_{\mathrm{s}}(-\mathbf{f}_{\mathrm{e}}) \tag{1}$$

where $\boldsymbol{\xi} = [\boldsymbol{\nu}_{\mathrm{e}}^{\mathrm{T}}, \mathbf{w}_{\mathrm{b}}^{\mathrm{T}}]^{\mathrm{T}}$. The matrices $\mathbf{M}_{\mathrm{s}} \in \mathbb{R}^{(6+3)\times(6+3)}$, $\mathbf{c}_{\mathrm{s}} \in \mathbb{R}^{(6+3)}$, $\mathbf{J}_{\mathrm{s}} \in \mathbb{R}^{(6+3)\times 6}$ and $\mathbf{A} \in \mathbb{R}^{(m+3)\times(6+3)}$ are defined in [8]. $\mathbf{f}_{\mathrm{e}} = [\mathbf{F}_{\mathrm{e}}^{\mathrm{T}}, \tau_{\mathrm{e}}^{\mathrm{T}}]^{\mathrm{T}} \in \mathbb{R}^6$ represents the force/torque at the end-effector where $\mathbf{F}_{\mathrm{e}} \in \mathbb{R}^3$ denotes the force and $\tau_{\mathrm{e}} \in \mathbb{R}^3$ denotes the torque. $\boldsymbol{\tau} = [\boldsymbol{\tau}_{\mathrm{m}}^{\mathrm{T}}, \boldsymbol{\tau}_{\mathrm{b}}^{\mathrm{T}}]^{\mathrm{T}}$, where $\boldsymbol{\tau}_{\mathrm{m}} \in \mathbb{R}^m$ denotes the manipulator's joint torques and $\boldsymbol{\tau}_{\mathrm{b}}$ is the control torque to be applied by the servicer's base attitude control system.

The target is modelled as a single rigid body where $\boldsymbol{\nu}_\mathrm{t} = [\mathbf{v}_\mathrm{t}^\mathrm{T}, \mathbf{w}_\mathrm{t}^\mathrm{T}]^\mathrm{T} \in \mathbb{R}^6$ represents the target's center of mass linear and angular velocity. The equation of motion of the target is given by:

$$\mathbf{M}_\mathrm{t}\dot{\boldsymbol{\nu}}_\mathrm{t} + \mathbf{c}_\mathrm{t} = \mathbf{J}_\mathrm{t}^\mathrm{T}(\mathbf{f}_\mathrm{e}) \tag{2}$$

where $\mathbf{M}_\mathrm{t} \in \mathbb{R}^{6\times6}$, $\mathbf{c}_\mathrm{t} \in \mathbb{R}^6$ and $\mathbf{J}_\mathrm{t} \in \mathbb{R}^{6\times6}$ are defined as:

$$\mathbf{M}_\mathrm{t} = \begin{bmatrix} m_\mathrm{t}\mathbf{E}_3 & \mathbf{0} \\ \mathbf{0} & \mathbf{I}_\mathrm{t} \end{bmatrix} \qquad \mathbf{c}_\mathrm{t} = \begin{bmatrix} \mathbf{0} \\ \mathbf{w}_\mathrm{t} \times \mathbf{I}_\mathrm{t}\mathbf{w}_\mathrm{t} \end{bmatrix} \qquad \mathbf{J}_\mathrm{t} = \begin{bmatrix} \mathbf{E}_3 & -\mathbf{r}_\mathrm{te}^\times \\ \mathbf{0} & \mathbf{E}_3 \end{bmatrix} \tag{3}$$

where m_t and $\mathbf{I}_\mathrm{t} \in \mathbb{R}^{3\times3}$ are the mass and inertia tensor of the target, respectively. $\mathbf{r}_\mathrm{te} \in \mathbb{R}^3$ is the radial vector from the target's center of mass to the grasping point.

The velocity of the end-effector and target are subjected to the following kinematic constraints as a result of grasping: $\boldsymbol{\nu}_\mathrm{e} = \mathbf{J}_\mathrm{t}\boldsymbol{\nu}_\mathrm{t}$ and $\dot{\boldsymbol{\nu}}_\mathrm{e} = \mathbf{J}_\mathrm{t}\dot{\boldsymbol{\nu}}_\mathrm{t} + \dot{\mathbf{J}}_\mathrm{t}\boldsymbol{\nu}_\mathrm{t}$. Making use of these constraints in (2), the target's dynamics can be expressed as:

$$\Lambda_\mathrm{t}\dot{\boldsymbol{\nu}}_\mathrm{e} - \Lambda_\mathrm{t}\dot{\mathbf{J}}_\mathrm{t}\mathbf{J}_\mathrm{t}^{-1}\boldsymbol{\nu}_\mathrm{e} + \mathbf{J}_\mathrm{t}^{-\mathrm{T}}\mathbf{c}_\mathrm{t} = \mathbf{f}_\mathrm{e} \tag{4}$$

where $\Lambda_t = \mathbf{J}_\mathrm{t}^{-\mathrm{T}}\mathbf{M}_\mathrm{t}\mathbf{J}_\mathrm{t}^{-1}$ represents the target's inertia projected onto the end-effector. The equation of motion of the combined servicer and target system is obtained by substituting (4) into (1), resulting in the following:

$$\bar{\mathbf{M}}\dot{\boldsymbol{\xi}} + \bar{\mathbf{c}} = \mathbf{A}^\mathrm{T}\tau \tag{5}$$

where $\bar{\mathbf{M}} = \mathbf{M}_\mathrm{s} + [\mathbf{J}_\mathrm{s}\Lambda_\mathrm{t}\ \mathbf{0}]$ and $\bar{\mathbf{c}} = \mathbf{c}_\mathrm{s} + \mathbf{J}_\mathrm{s}(\mathbf{J}_\mathrm{t}^{-\mathrm{T}}\mathbf{c}_\mathrm{t} - \Lambda_\mathrm{t}\dot{\mathbf{J}}_\mathrm{t}\mathbf{J}_\mathrm{t}^{-1}\boldsymbol{\nu}_\mathrm{e})$. Equation (5) will be used for control purposes.

3 Robust Trajectory Tracking Controller

This section presents the servicer's controller development to simultaneously track a desired end-effector detumbling trajectory and to regulate the servicer's base attitude with an unknown target attached to the end-effector. The controller's development does not require force/torque measurements at the end-effector and takes into account magnitude constraints on the servicer's control inputs. To achieve this the position and orientation error of the end-effector and base attitude, along with the end-effector and base velocity errors are defined as follows:

$$\mathbf{e}_\mathrm{P} = \begin{bmatrix} \mathbf{x}_\mathrm{e} - \mathbf{x}_\mathrm{e}^\mathrm{d} \\ (\delta\mathbf{q}_\mathrm{v})_\mathrm{e} \\ (\delta\mathbf{q}_\mathrm{v})_\mathrm{b} \end{bmatrix} = \begin{bmatrix} \mathbf{e}_\mathrm{pe} \\ (\delta\mathbf{q}_\mathrm{v})_\mathrm{e} \\ (\delta\mathbf{q}_\mathrm{v})_\mathrm{b} \end{bmatrix} \qquad \mathbf{e}_\mathrm{V} = \begin{bmatrix} \mathbf{v}_\mathrm{e} - \mathbf{v}_\mathrm{e}^\mathrm{d} \\ \mathbf{w}_\mathrm{e} - \mathbf{w}_\mathrm{e}^\mathrm{d} \\ \mathbf{w}_\mathrm{b} - \mathbf{w}_\mathrm{b}^\mathrm{d} \end{bmatrix} = \begin{bmatrix} \mathbf{e}_\mathrm{ve} \\ \mathbf{e}_\mathrm{we} \\ \mathbf{e}_\mathrm{wb} \end{bmatrix} \tag{6}$$

where $(\delta\mathbf{q}_\mathrm{v})_{(\cdot)}$ denote the vector component of the quaternion associated with the attitude tracking error of the end-effector, $(\cdot) = \mathrm{e}$, and base, $(\cdot) = \mathrm{b}$. $\delta\mathbf{q}_\mathrm{v} = \mathrm{q_s}\mathbf{q}_\mathrm{v}^\mathrm{d} + \mathbf{q}_\mathrm{v} \times \mathbf{q}_\mathrm{v}^\mathrm{d} - \mathbf{q}_\mathrm{v}\mathrm{q}_\mathrm{s}^\mathrm{d} \in \mathbb{R}^3$ where the scalar and vector components of the quaternion are denoted by $(\cdot)_\mathrm{s}$ and $(\cdot)_\mathrm{v}$, respectively, and $(\cdot)^\mathrm{d}$ represents the desired quaternion value. Making use of (6), a sliding variable, $\mathbf{s}_1 \in \mathbb{R}^9$, is defined as:

$$\mathbf{s}_1 = \mathbf{e}_\mathrm{V} + \mathbf{K}_\mathrm{P}\mathbf{e}_\mathrm{P} \tag{7}$$

where $\mathbf{K}_\mathrm{P} = \mathrm{diag}[\mathbf{K}_\mathrm{PEL}, \mathrm{K}_\mathrm{PEA}\mathbf{E}_3, \mathrm{K}_\mathrm{PBA}\mathbf{E}_3]$ and $0 < \mathbf{K}_\mathrm{PEL} \in \mathbb{R}^{3\times3}$, $\mathrm{K}_\mathrm{PEA} \in \mathbb{R}$ and $\mathrm{K}_\mathrm{PBA} \in \mathbb{R}$ are positive gains. Let $\mathbf{s}_1 = [\mathbf{s}_\mathrm{1pe}^\mathrm{T}, \mathbf{s}_\mathrm{1we}^\mathrm{T}, \mathbf{s}_\mathrm{1wb}^\mathrm{T}]^\mathrm{T}$ where $\mathbf{s}_\mathrm{1pe} \in \mathbb{R}^3$, $\mathbf{s}_\mathrm{1we} \in \mathbb{R}^3$ and $\mathbf{s}_\mathrm{1wb} \in \mathbb{R}^3$. It follows from (6) and (7) that:

$$\mathbf{s}_\mathrm{1pe} = \mathbf{e}_\mathrm{ve} + \mathbf{K}_\mathrm{PEL}\mathbf{e}_\mathrm{pe}; \qquad \mathbf{s}_\mathrm{1we} = \mathbf{e}_\mathrm{we} + \mathrm{K}_\mathrm{PEA}(\delta\mathbf{q}_\mathrm{v})_\mathrm{e}; \qquad \mathbf{s}_\mathrm{1wb} = \mathbf{e}_\mathrm{wb} + \mathrm{K}_\mathrm{PBA}(\delta\mathbf{q}_\mathrm{v})_\mathrm{b} \tag{8}$$

Boundedness of $\mathbf{s}_1$ will result in $\mathbf{e}_\mathrm{V}$ and $\mathbf{e}_\mathrm{P}$ also being ultimately bounded. For the first system in (8), this follows since it represents an exponentially stable system that is disturbed by an ultimately bounded input in $\mathbf{s}_{1\mathrm{pe}}$. Similarly, boundedness of $\mathbf{e}_{\mathrm{w}(\cdot)}$ and $(\delta\mathbf{q}_\mathrm{v})_{(\cdot)}$ for a bounded $\mathbf{s}_{1\mathrm{w}(\cdot)}$ in the second and third systems described in (8) where $(\cdot)=\mathrm{e}$ and $(\cdot)=\mathrm{b}$, respectively, follows from Lemma 1 in [16].

The controller design takes into account magnitude constraints on the servicer's control inputs by modelling the servicer's control inputs, τ in (5), by a smooth hyperbolic tangent function [23]:

$$\tau = f(\mathbf{V}); \qquad \{f(\mathbf{V})\}_i = \{\mathbf{U}_\mathrm{M}\}_i \tanh(\{\mathbf{V}\}_i/\{\mathbf{U}_\mathrm{M}\}_i) \tag{9a}$$

$$\dot{\boldsymbol{V}} = \bar{f}^{-1}\mathbf{U} \tag{9b}$$

where $i = 1,2,3,...,(m+3)$ and the i^{th} element of $\mathbf{U}_\mathrm{M} \in \mathbb{R}^{(m+3)}$ denotes the control input magnitude limit of the i^{th} servicer's actuator. $\bar{f} = \partial f/\partial \mathbf{V}$, $\mathbf{V} \in \mathbb{R}^{m+3}$ and $\mathbf{U} \in \mathbb{R}^{m+3}$. From the above model of the servicer's control input, it can be concluded that servicer's control input will always satisfies its magnitude constraint: $\{\tau\}_i \leq \{\mathbf{U}_\mathrm{M}\}_i$ for $i = 1,2,3,...,(m+3)$. All functions of the resultant system comprising of (5) and (9) are smooth, and hence, the use of the backstepping technique is feasible to design the auxiliary signal $\mathbf{U}$. The use of the hyperbolic tangent function to model the servicer's control inputs is an alternative to the use of a discontinuous auxiliary system designed to account for control input magnitude limits as in [10]. The latter adds additional complexity in the tuning of the auxiliary system and analysis of the resultant controller, while the former results in a simpler control design and analysis of the resultant controller with the use of the backstepping technique. The design of $\mathbf{U}$ is described in the following steps:

Step 1: Design of the virtual controller for $f(\mathbf{V})$. The dynamic equation for $\mathbf{s}_1$ is obtain using (7) and (5):

$$\bar{\mathbf{M}}_\mathrm{o}\dot{\mathbf{s}}_1 = \mathbf{A}^\mathrm{T} f(\mathbf{V}) - \bar{\mathbf{c}}_\mathrm{o} - \Delta\bar{\mathbf{c}} - \bar{\mathbf{M}}_\mathrm{o}\dot{\xi}^\mathrm{d} - \Delta\bar{\mathbf{M}}\dot{\xi} + \bar{\mathbf{M}}_\mathrm{o}\mathbf{K}_\mathrm{P}\dot{\mathbf{e}}_\mathrm{p} \tag{10}$$

where $\bar{\mathbf{M}}_\mathrm{o} = \mathbf{M}_\mathrm{s}$ and $\bar{\mathbf{c}}_\mathrm{o} = \mathbf{c}_\mathrm{s}$ denote the nominal component of the servicer/target mass matrix and nominal component of the servicer's nonlinear velocity dependent terms, respectively. $\Delta\bar{\mathbf{M}} = [\mathbf{J}_\mathrm{s}\Lambda_\mathrm{t}\ \mathbf{0}] \in \mathbb{R}^{(6+3)\times(6+3)}$ and $\Delta\bar{\mathbf{c}} = \mathbf{J}_\mathrm{s}(\mathbf{J}_\mathrm{t}^{-\mathrm{T}}\mathbf{c}_\mathrm{t} - \Lambda_\mathrm{t}\dot{\mathbf{J}}_\mathrm{t}\mathbf{J}_\mathrm{t}^{-1}\boldsymbol{v}_\mathrm{e})$ so that $\bar{\mathbf{M}} = \bar{\mathbf{M}}_\mathrm{o} + \Delta\bar{\mathbf{M}}$ and $\bar{\mathbf{c}} = \bar{\mathbf{c}}_\mathrm{o} + \Delta\bar{\mathbf{c}}$.

Utilizing the definition of Λ_t, $\mathbf{J}_\mathrm{t}$ and $\mathbf{c}_\mathrm{t}$ in Section 2.2, the evaluation of $\Delta\bar{\mathbf{c}}$ is as follows:

$$\begin{aligned}\Delta\bar{\mathbf{c}} &= \mathbf{J}_\mathrm{s}(\mathbf{J}_\mathrm{t}^{-\mathrm{T}}\mathbf{c}_\mathrm{t} - \Lambda_\mathrm{t}\dot{\mathbf{J}}_\mathrm{t}\mathbf{J}_\mathrm{t}^{-1}\boldsymbol{v}_\mathrm{e}) \\ &= \mathbf{J}_\mathrm{s}\begin{bmatrix} m_\mathrm{t}\dot{\mathbf{r}}_\mathrm{te}^{\times}\mathbf{w}_\mathrm{t} \\ \mathbf{w}_\mathrm{t}\times\mathbf{I}_\mathrm{t}\mathbf{w}_\mathrm{t} - m_\mathrm{t}\mathbf{r}_\mathrm{te}^{\times}\dot{\mathbf{r}}_\mathrm{te}^{\times}\mathbf{w}_\mathrm{t}\end{bmatrix} \\ &= \mathbf{J}_\mathrm{s}(\gamma_1+\gamma_2)\end{aligned} \tag{11}$$

where with the use of $\mathbf{w}_\mathrm{t} = \mathbf{w}_\mathrm{e} = \mathbf{e}_\mathrm{we} + \mathbf{w}_\mathrm{e}^\mathrm{d}$ in (11), γ_1 and γ_2 are defined as follows:

$$\gamma_1 = \begin{bmatrix} m_\mathrm{t}\mathbf{w}_\mathrm{t}^{\mathrm{d}\times}\mathbf{r}_\mathrm{te}^{\times}\mathbf{w}_\mathrm{t}^\mathrm{d} \\ \mathbf{w}_\mathrm{t}^\mathrm{d}\times\mathbf{I}_\mathrm{t}\mathbf{w}_\mathrm{t}^\mathrm{d} - m_\mathrm{t}\mathbf{r}_\mathrm{te}^{\times}\mathbf{w}_\mathrm{t}^{\mathrm{d}\times}\mathbf{r}_\mathrm{te}^{\times}\mathbf{w}_\mathrm{t}^\mathrm{d}\end{bmatrix} \qquad \gamma_2 = \begin{bmatrix} m_\mathrm{t}\gamma_{2\mathrm{a}} \\ \gamma_{2\mathrm{b}} + m_\mathrm{t}\mathbf{r}_\mathrm{te}^{\times}\gamma_{2\mathrm{a}}\end{bmatrix} \tag{12}$$

where $\gamma_{2\mathrm{a}} = \mathbf{e}_\mathrm{we}^{\times}\mathbf{r}_\mathrm{te}^{\times}\mathbf{e}_\mathrm{we} + 2\mathbf{e}_\mathrm{we}^{\times}\mathbf{r}_\mathrm{te}^{\times}\mathbf{w}_\mathrm{e}^\mathrm{d}$ and $\gamma_{2\mathrm{b}} = \mathbf{e}_\mathrm{we}\times\mathbf{I}_\mathrm{t}\mathbf{e}_\mathrm{we} + \mathbf{e}_\mathrm{we}\times\mathbf{I}_\mathrm{t}\mathbf{w}_\mathrm{e}^\mathrm{d} + \mathbf{w}_\mathrm{e}^\mathrm{d}\times\mathbf{I}_\mathrm{t}\mathbf{e}_\mathrm{we}$.

The target's inertial parameters are upper bounded as follows: $m_\mathrm{t} \leq m_\mathrm{tU}$, $\lambda_{\min}(\mathbf{I}_\mathrm{t}) \leq \|\mathbf{I}_\mathrm{t}\| \leq \lambda_{\max}(\mathbf{I}_\mathrm{t})$ and $\|\mathbf{r}_\mathrm{te}\| \leq \mathrm{r}_\mathrm{teU}$. Using bounds on the target's inertial parameters and Lemma 1 in [23] results in the following bounds on the components of γ_1 in (12) as: $\|m_\mathrm{t}\mathbf{w}_\mathrm{t}^{\mathrm{d}\times}\mathbf{r}_\mathrm{te}^{\times}\mathbf{w}_\mathrm{t}^\mathrm{d}\| \leq m_\mathrm{tU}\mathrm{r}_\mathrm{teU}\|\mathbf{w}_\mathrm{e}^\mathrm{d}\|^2$, $\|\mathbf{w}_\mathrm{t}^\mathrm{d}\times\mathbf{I}_\mathrm{t}\mathbf{w}_\mathrm{t}^\mathrm{d}\| \leq (\lambda_{\max}^2(\mathbf{I}_\mathrm{t}) - \lambda_{\min}^2(\mathbf{I}_\mathrm{t}))^{1/2}\|\mathbf{w}_\mathrm{e}^\mathrm{d}\|^2$ and

$\|m_{\mathrm{t}}\mathbf{r}_{\mathrm{te}}^{\times}\mathbf{w}_{\mathrm{t}}^{\mathrm{d}\times}\mathbf{r}_{\mathrm{te}}^{\times}\mathbf{w}_{\mathrm{t}}^{\mathrm{d}}\| \leq m_{\mathrm{tU}}\mathrm{r}_{\mathrm{teU}}^{2}\|\mathbf{w}_{\mathrm{e}}^{\mathrm{d}}\|^{2}$. Making use of these bounds the magnitude of γ_1 is upper bounded as:

$$\|\gamma_1\| \leq h\|\mathbf{w}_{\mathrm{e}}^{\mathrm{d}}\|^{2} \tag{13}$$

where $h = [(m_{\mathrm{tU}}\mathrm{r}_{\mathrm{teU}})^2 + ([\lambda_{\max}^2(\mathbf{I}_{\mathrm{t}}) - \lambda_{\min}^2(\mathbf{I}_{\mathrm{t}})]^{1/2} + m_{\mathrm{tU}}\mathrm{r}_{\mathrm{teU}}^2)^2]^{1/2}$. Furthermore, with the use of (13), $\mathbf{J}_{\mathrm{s}}\gamma_1$ can be upper bounded as follows:

$$\|\mathbf{J}_{\mathrm{s}}\gamma_1\| \leq h\|\mathbf{J}_{\mathrm{s}}\|\|\mathbf{w}_{\mathrm{e}}^{\mathrm{d}}\|^{2} \leq \theta. \tag{14}$$

where θ is known positive constant since h can be computed utilizing bounds on the target's inertial parameters, $\mathbf{J}_{\mathrm{s}}$ is a function of known servicer's inertial and geometric parameters [7, 8], and $\mathbf{w}_{\mathrm{e}}^{\mathrm{d}}$ can be designed to be bounded as per the design of the desired detumbling trajectory.

To design the virtual controller for $f(\mathbf{V})$, we utilize the following Lyapunov function candidate from [23] which is radially unbounded and globally positive-definite function:

$$\mathrm{V}_1 = \textstyle\sum_{i=1}^{9} \ln(\cosh(\{\mathbf{s}_1\}_i)) \tag{15}$$

Taking the time derivative of (15) and making use of (10) and (11), results in the following expression for $\dot{\mathrm{V}}_1$:

$$\dot{\mathrm{V}}_1 = \tanh^{\mathrm{T}}(\mathbf{s}_1)\bar{\mathbf{M}}_{\mathrm{o}}^{-1}(\mathbf{A}^{\mathrm{T}}f(\mathbf{V}) - \bar{\mathbf{c}}_{\mathrm{o}} - \mathbf{J}_{\mathrm{s}}(\gamma_1+\gamma_2) - \bar{\mathbf{M}}_0\dot{\boldsymbol{\xi}}^{\mathrm{d}} - \Delta\bar{\mathbf{M}}\dot{\boldsymbol{\xi}} + \bar{\mathbf{M}}_{\mathrm{o}}\mathbf{K}_{\mathrm{P}}\dot{\mathbf{e}}_{\mathrm{p}}) \tag{16}$$

where $\tanh(\mathbf{x}) = [\tanh(x_1), \tanh(x_2), ..., \tanh(x_n)]^{\mathrm{T}}$ for any vector $\mathbf{x} \in \mathbb{R}^n$

Considering $f(\mathbf{V})$ as a virtual controller, the following virtual controller is proposed:

$$f(\mathbf{V})^{\mathrm{d}} = \mathbf{A}^{-\mathrm{T}}(\bar{\mathbf{c}}_{\mathrm{o}} + \bar{\mathbf{M}}_{\mathrm{o}}\dot{\boldsymbol{\xi}}^{\mathrm{d}} - \bar{\mathbf{M}}_{\mathrm{o}}\mathbf{K}_{\mathrm{P}}\dot{\mathbf{e}}_{\mathrm{P}} - \bar{\mathbf{M}}_{\mathrm{o}}\mathrm{K}_1\tanh(\mathbf{s}_1) - \boldsymbol{\psi}_1) \tag{17}$$

with K_1 as a positive constant and $\boldsymbol{\psi}_1 \in \mathbb{R}^9$ is a robust compensator defined as in [9]:

$$\psi_{1i} = \theta\tanh\Big(\tfrac{9\mathrm{k}_u\theta\{\bar{\mathbf{M}}_{\mathrm{o}}^{-1}\tanh(\mathbf{s}_1)\}_i}{\varepsilon_1}\Big) \qquad \text{for } i = 1,2,3,...,9 \tag{18}$$

where $\mathrm{k}_u = 0.2785$ [15] and ε_1 is a small positive scalar. The hyperbolic tangent function has the following property [15]:

$$0 \leq |x| - x\tanh\big(x/\varepsilon_{\mathrm{u}}\big) \leq \mathrm{k}_{\mathrm{u}}\varepsilon_u \tag{19}$$

for any $\varepsilon_{\mathrm{u}} > 0$ and any $x \in \mathbb{R}$. Making use of this property, the following bound is obtained: $\|\tanh^{\mathrm{T}}(\mathbf{s}_1)\bar{\mathbf{M}}_{\mathrm{o}}^{-1}\|\theta - \tanh^{\mathrm{T}}(\mathbf{s}_1)\bar{\mathbf{M}}_{\mathrm{o}}^{-1}\psi_1 \leq \sum_1^9 \big(|\{\tanh^{\mathrm{T}}(\mathbf{s}_1)\bar{\mathbf{M}}_{\mathrm{o}}^{-1}\}_i|\theta - \{\tanh^{\mathrm{T}}(\mathbf{s}_1)\bar{\mathbf{M}}_{\mathrm{o}}^{-1}\}_i\{\psi_1\}_i\big) \leq \varepsilon_1$. Using this bound and (17) in (16), results in:

$$\begin{aligned}\dot{\mathrm{V}}_1 &= \tanh^{\mathrm{T}}(\mathbf{s}_1)\bar{\mathbf{M}}_{\mathrm{o}}^{-1}(\mathbf{A}^{\mathrm{T}}\mathbf{s}_2 + \mathbf{A}^{\mathrm{T}}f(\mathbf{V})^{\mathrm{d}} - \bar{\mathbf{c}}_{\mathrm{o}} - \mathbf{J}_{\mathrm{s}}(\gamma_1+\gamma_2) - \bar{\mathbf{M}}_{\mathrm{o}}\dot{\boldsymbol{\xi}} + \bar{\mathbf{M}}_{\mathrm{o}}\mathbf{K}_{\mathrm{P}}\dot{\mathbf{e}}_{\mathrm{P}} - \Delta\bar{\mathbf{M}}\dot{\boldsymbol{\xi}}) \\ &\leq -\mathrm{K}_1\|\tanh(\mathbf{s}_1)\|^2 + \varepsilon_1 + \tanh^{\mathrm{T}}(\mathbf{s}_1)\boldsymbol{\chi}\end{aligned} \tag{20}$$

where $\mathbf{s}_2 = f(\mathbf{V}) - f(\mathbf{V})^{\mathrm{d}}$ and $\boldsymbol{\chi} = \bar{\mathbf{M}}_{\mathrm{o}}^{-1}(\mathbf{A}^{\mathrm{T}}\mathbf{s}_2 - \mathbf{J}_{\mathrm{s}}\gamma_2 - \Delta\bar{\mathbf{M}}\dot{\boldsymbol{\xi}})$.

Step 2: Design the control law for the input $\mathbf{U}$ to the auxiliary system, (9b). Using (9), the dynamic equation for $\mathbf{s}_2$ is obtained as follows:

$$\dot{\mathbf{s}}_2 = \dot{f}(\mathbf{V}) - \dot{f}(\mathbf{V})^{\mathrm{d}} = \mathbf{U} - \dot{f}(\mathbf{V})^{\mathrm{d}} \tag{21}$$

The input $\mathbf{U}$ to the auxiliary system (9b), is designed to robustly compensate for $\dot{f}(\mathbf{V})^{\mathrm{d}}$. To achieve this, we construct the following compact sets:

$$\Omega_1 = \left\{ \|\mathbf{x}_{\mathrm{e}}^{\mathrm{d}}\| \leq \mathrm{C}_1, \|\xi^{\mathrm{d}}\| \leq \mathrm{C}_2, \|\dot{\xi}^{\mathrm{d}}\| \leq \mathrm{C}_3, \|\ddot{\xi}^{\mathrm{d}}\| \leq \mathrm{C}_4 \right\} \tag{22a}$$

$$\Omega_2 = \left\{ (\mathbf{s}_1, \mathbf{s}_2) \;\middle|\; \textstyle\sum_{i=1}^{9} \ln(\cosh(\{\mathbf{s}_1\}_i)) + \sum_{i=1}^{m+3} \ln(\cosh(\{\mathbf{s}_2\}_i)) \leq \mathrm{C}_5 \right\} \tag{22b}$$

where $\mathrm{C}_{i=1,2,3,4,5}$ are positive constants. The desired detumbling trajectory is determined by the controller designer such that the selection C_1 to C_4 can be made to satisfy (22a). The choice of C_5 is free but will affect the controller's gain selection as discussed at the end of this Section. Furthermore, provided that $\mathbf{s}_1$ and $\mathbf{s}_2$ are contained in the compact set Ω_2, with the use of Corollary 1, it follows that χ and $\dot{f}(\mathbf{V})^{\mathrm{d}}$ are bounded, such that $\|\chi\| \leq \mathrm{M}_1$ and $\|\dot{f}(\mathbf{V})^{\mathrm{d}}\| \leq \mathrm{M}_2$ where $\mathrm{M}_{i=1,2}$ are positive constants. From this, the control law for $\mathbf{U}$ is proposed as:

$$\mathbf{U} = -\mathrm{K}_2 \tanh(\mathbf{s}_2) - \psi_2 \tag{23}$$

where K_2 is a positive constant and ψ_2 is a robust compensator that is defined as [9]:

$$\psi_{2i} = \hat{\mathrm{M}}_2 \tanh\left(\tfrac{(m+3)\mathrm{k}_u \hat{\mathrm{M}}_2 \{\tanh(\mathbf{s}_2)\}_i}{\varepsilon_1}\right) \qquad \text{for } i = 1, 2, 3, ..., (m+3) \tag{24}$$

The variable $\hat{\mathrm{M}}_2$ is an estimate of M_2 and is updated by the following update law [23]:

$$\dot{\hat{\mathrm{M}}}_2 = \sigma_1 \|\tanh(\mathbf{s}_2)\| - \sigma_1 \sigma_2 \hat{\mathrm{M}}_2 \tag{25}$$

Uniform ultimate boundedness of $\mathbf{s}_1$, $\mathbf{s}_2$ and $\tilde{\mathrm{M}}_2 = \mathrm{M}_2 - \hat{\mathrm{M}}_2$ can be concluded with the use of the following Lyapunov function candidate:

$$\mathrm{V} = \mathrm{V}_1 + \textstyle\sum_{i=1}^{m+3} \ln(\cosh(\{\mathbf{s}_2\}_i)) + \frac{1}{2\sigma_1} \tilde{\mathrm{M}}_2^2 \tag{26}$$

The time derivative of (26) along with (20), (21) and (23-25) results in the following:

$$\begin{aligned}
\dot{\mathrm{V}} &\leq -\mathrm{K}_1 \|\tanh(\mathbf{s}_1)\|^2 - \mathrm{K}_2 \|\tanh(\mathbf{s}_2)\|^2 + \varepsilon_1 + \tanh^{\mathrm{T}}(\mathbf{s}_1)\chi + \tanh^{\mathrm{T}}(\mathbf{s}_2)(-\dot{f}(\mathbf{V})^{\mathrm{d}} - \psi_2) \\
&\quad - (1/\sigma_1)\tilde{\mathrm{M}}_2 \dot{\hat{\mathrm{M}}}_2 \\
&\leq -\mathrm{K}_1 \|\tanh(\mathbf{s}_1)\|^2 - \mathrm{K}_2 \|\tanh(\mathbf{s}_2)\|^2 + \varepsilon_1 + \mathrm{M}_1 - \tanh^{\mathrm{T}}(\mathbf{s}_2)\psi_2 + \|\tanh^{\mathrm{T}}(\mathbf{s}_2)\|(\mathrm{M}_2 - \hat{\mathrm{M}}_2) \\
&\quad + \|\tanh^{\mathrm{T}}(\mathbf{s}_2)\|\hat{\mathrm{M}}_2 - (1/\sigma_1)\tilde{\mathrm{M}}_2 \dot{\hat{\mathrm{M}}}_2 \\
&\leq -\mathrm{K}_1 \|\tanh(\mathbf{s}_1)\|^2 - \mathrm{K}_2 \|\tanh(\mathbf{s}_2)\|^2 + 2\varepsilon_1 + \mathrm{M}_1 + \|\tanh^{\mathrm{T}}(\mathbf{s}_2)\|(\mathrm{M}_2 - \hat{\mathrm{M}}_2) - (1/\sigma_1)\tilde{\mathrm{M}}_2 \dot{\hat{\mathrm{M}}}_2 \\
&\leq -\mathrm{K}_1 \|\tanh(\mathbf{s}_1)\|^2 - \mathrm{K}_2 \|\tanh(\mathbf{s}_2)\|^2 - (\sigma_2/2)\tilde{\mathrm{M}}_2^2 + \bar{\varepsilon}
\end{aligned} \tag{27}$$

where the following inequalities were utilized in (27): $\hat{\mathrm{M}}_2 \|\tanh(\mathbf{s}_2)\| - \tanh^{\mathrm{T}}(\mathbf{s}_2)\psi_2 \leq \varepsilon_1$, $\sigma_2 \tilde{\mathrm{M}}_2 \hat{\mathrm{M}}_2 \leq -\frac{\sigma_2}{2}\tilde{\mathrm{M}}_2^2 + \frac{\sigma_2}{2}\mathrm{M}_2^2$, and $\bar{\varepsilon} = 2\varepsilon_1 + \mathrm{M}_1 + \frac{\sigma_2}{2}\mathrm{M}_2^2$.

From (27), $\dot{\mathrm{V}}$ can be expressed as:

$$\dot{\mathrm{V}} \leq -\rho \bar{\mathrm{V}} + \bar{\varepsilon}; \qquad \bar{\mathrm{V}} = \|\tanh(\mathbf{s}_1)\|^2 + \|\tanh(\mathbf{s}_2)\|^2 + \tilde{\mathrm{M}}_2^2 \tag{28}$$

where $\rho = \min\{\mathrm{K}_1, \mathrm{K}_2, \sigma_2/2\}$. Thus, $\dot{\mathrm{V}}$ is strictly negative outside the following compact set: $\Omega_3 = \left\{ \bar{\mathrm{V}} \;\middle|\; \bar{\mathrm{V}} \leq \bar{\varepsilon}/\rho \right\}$. From this, we can conclude that $\mathbf{s}_1$, $\mathbf{s}_2$ and $\tilde{\mathrm{M}}_2$ are uniformly ultimately bounded provided that $\mathrm{V}(0) \leq \mathrm{C}_5$ and the controller gains, K_1, K_2 and σ_2 be chosen such that $\rho > \bar{\varepsilon}/\bar{\mathrm{p}}$, where $\bar{\mathrm{p}} = \min_{\mathrm{V}=\mathrm{C}_5} \bar{\mathrm{V}}$. The size of set Ω_3 is determined by the gains K_1, K_2, ε_1 and σ_2, and reflects the final bound on $\mathbf{s}_1$, $\mathbf{s}_2$ and $\tilde{\mathrm{M}}_2$. A smaller bound requires higher selection of the gains K_1, K_2 and σ_2 with a lower ε_1.

Table 1 7-DOF Model Parameters

	Mass(kg)	I_{xx}(kgm^2)	I_{yy}(kgm^2)	I_{zz}(kgm^2)
Base	1000	1200	1200	1200
Link 1	35.01	1.218	0.5132	1.331
Link 2	30	2.10	1.378	2.359
Link 3	22.69	0.102	3.378	3.359
Link 4	21.38	0.4327	2.266	1.911
Link 5	16.75	0.3878	0.3963	0.07271
Link 6	26.17	0.5727	0.5987	0.1288
Link 7	18.07	0.165	0.241	0.135

4 Numerical Simulation Study

This section presents the evaluation of the proposed robust controller to track a desired detumbling trajectory in order to detumble a non-cooperative target with uncertain but bounded inertial parameters. The evaluation is carried out using a 7-degree-of-freedom (DOF) space manipulator servicer satellite that is based on a modified model of ETS-VII system (model parameters are presented in Table 1 and Denavit-Hartenberg parameters found in [12]). The target is a cube with 0.5m sides where $m_{\mathrm{t}} = 40$kg and $\mathbf{I}_{\mathrm{t}} = diag([16,25,25])$kgm^2.

The target is grasped at $t = 0$s, resulting in a redistribution of its momentum in the servicer-target system. The velocities of the servicer-target system after grasping ($t^+ = 0$s) are computed as in [19]. The target has an initial angular velocity of $\mathbf{w}_{\mathrm{t}} = [4,\ 4,\ 5.7]^{\mathrm{T}}$deg/s at the start of the post grasping phase. Furthermore, functions from the SpaceDyn toolbox [20] were utilized to compute the servicer's mass matrix, Jacobian and nonlinear forces.

The desired end-effector's linear and angular velocity are described by: $\boldsymbol{\nu}_{\mathrm{e}}^{\mathrm{d}} = (1+(e^{-\tau_{\mathrm{n}}} - 0.5e^{-1}\tau_{\mathrm{n}}^2 + 2e^{-1}\tau_{\mathrm{n}} - 1)/(1-2.5e^{-1}))\boldsymbol{\nu}_{\mathrm{e(int)}}$, where $\boldsymbol{\nu}_{\mathrm{e(int)}}$ denotes the end-effector's velocity at the start of the post-grasping phase and $\tau_{\mathrm{n}} \in [0,1]$ denotes normalized time where $\dot{\tau}_{\mathrm{n}} = 0.3$. From this, the desired end-effector position and orientation and acceleration can be determined. Regulating the servicer's base attitude is not required in detumbling the target and the servicer's base desired angular velocity is set to zero.

Tracking the reference detumbling trajectory while robustly compensating for the unknown target is accomplished by applying the control input $\mathbf{U}$ in (23) to the augmented model for the servicer's input defined in (9b) in order to determine the variable $\mathbf{V}$. $\mathbf{V}$ is then utilized to compute the servicer's actuator torques, $\tau = f(\mathbf{V})$, where $f(\mathbf{V})$ is defined in (9a). The following controller gains are utilized: $\mathbf{K}_{PEL} = 0.2\mathbf{E}_3$, $\mathrm{K}_{PEA} = 0.1$, $\mathrm{K}_{PBA} = 0$, $\mathbf{K}_1 = 4$, $\mathbf{K}_2 = 2$, $\varepsilon_1 = 1$, $\sigma_1 = 10$, $\sigma_2 = 1$, $\{\mathbf{U}_{\mathrm{M}}\}_i = 2.5$Nm for $i = 1,2,3,...m$ (manipulator) and $\{\mathbf{U}_{\mathrm{M}}\}_i = 1.5$Nm for $i = (m+1),...(m+3)$ (base attitude control). Bounds on the target's inertial parameters are as follows: $\mathrm{r}_{\mathrm{teU}} = \sqrt{0.1875}$m, $m_{\mathrm{tU}} = 44$kg, $\lambda_{max}(\mathbf{I}_{\mathrm{t}}) = 28$kgm^2 and $\lambda_{min}(\mathbf{I}_{\mathrm{t}}) = 14.5$kgm^2. Furthermore, joint null space damping is utilized to minimize excess manipulator joint motion in the null space of the detumbling task.

The end-effector position and orientation errors are presented in the left plots in Fig. 1. The end-effector linear and angular velocity tracking error as well as the base angular velocity error are presented in the right plots in Fig. 1. As observed from these plots, the tracking errors converge to a neighbourhood of zero and remained there even as the servicer's base attitude control input were saturated (Fig. 2).

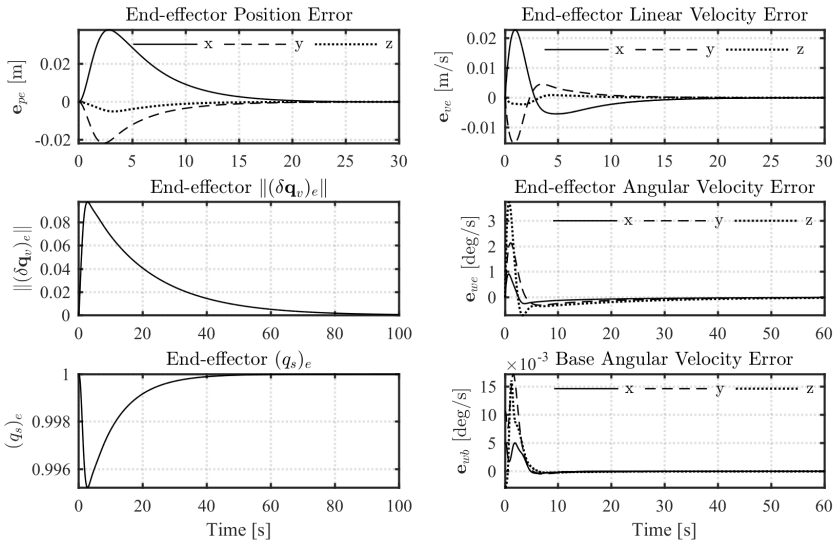

Fig. 1 Left plots: End-effector's position and orientation error. Right plots: End-effector's linear and angular velocity error and base angular velocity error.

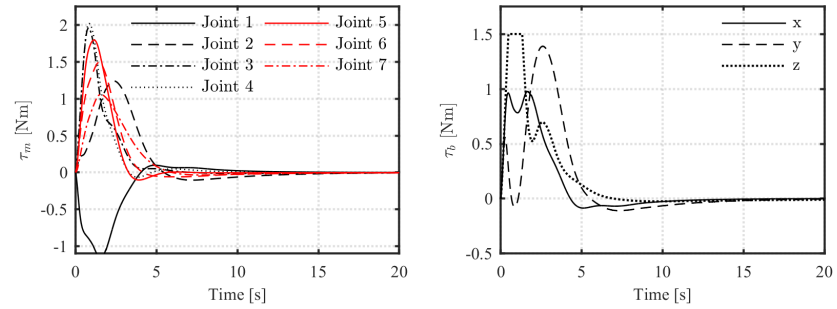

Fig. 2 Servicer's manipulator joint torque profile (left plot) and servicer's base attitude control torques (right plot). $\{\mathbf{U}_\mathrm{M}\}_i = 2.5$Nm for $i = 1,2,3,...m$ (manipulator, τ_m) and $\{\mathbf{U}_\mathrm{M}\}_i = 1.5$Nm for $i = (m+1),...(m+3)$ (base attitude control, τ_b)

5 Conclusion

This study presents a robust adaptive detumbling controller to detumble a non-cooperative target with unknown but bounded inertial parameters. The robust adaptive detumbling controller achieves detumbling of the target by tracking a desired detumbling trajectory while taking into account magnitude constraints on the servicer's control inputs. This is achieved by modelling the magnitude constraints on the servicer's control inputs with the use of the hyperbolic tangent function, which results in a system that is non-affine in its control inputs. Using an augmented model, bounds on the target's inertial parameters and robust adaptive control approach, the detumbling controller is designed with the use of the backsetepping technique. The performance of the proposed robust controller is examined through numerical simulations where it is demonstrated that detumbling of the target is accomplished even as the servcier's control input became saturated.

References

1. Abiko, S., Lampariello, R., Hirzinger, G.: Impedance control for a free-floating robot in the grasping of a tumbling target with parameter uncertainty. In: Proc. of IEEE/RSJ International Conference on Intell. Robots and Systems, pp. 1020–1025. Beijing (2006)
2. Aghili, F.: Coordination control of a free-fying manipulator and its base attitude to capture and detumble a non-cooperative satellite. In: Proc. of IEEE/RSJ International Conference on Intell. Robots and Systems, pp. 2365–2372 (2009)
3. Aghili, F.: Optimal control of a space manipulator for detumbling of a target satellite. In: Proc. of IEEE/RSJ International Conference on Intell. Robots and Automation, pp. 3019–3024. Kobe, Japan (2009)
4. Aghili, F.: A prediction and motion-planning scheme for visually guided robotic capturing of free-floating tumbling objects with uncertain dynamics. IEEE Transactions on Robotics **28**(3), 634–649 (2012)
5. Aghili, F.: Pre and post-grasping robot motion planning to capture and stabilize a tumbling/drifting free-floater with uncertain dynamics. In: Proc. of IEEE/RSJ International Conference on Intell. Robots and Automation, pp. 5461–5468. Karlsruhe, Germany (2013)
6. Dimitrov, D., Yoshida, Y.: Momentum distribution in a space manipulator for facilitating the post-impact control. In: Proc. of IEEE/RSJ International Conference on Intell. Robots and Systems, pp. 3345–3350. Sendai, Japan (2004)
7. Gangapersaud, R., Liu, G., de Ruiter, A.: Detumbling a non-cooperative space target with model uncertainties using a space manipulator. Journal of Guidance, Control, and Dynamics **42**(4), 910–918 (2019)
8. Gangapersaud, R., Liu, G., de Ruiter, A.: Detumbling of a non-cooperative target with unknown inertial parameters using a space robot. Advances in Space Research **63**(12), 3900–3915 (2019)
9. Hou, Z.G., Cheng, A.M., Tan, M.: Adaptive control of an electrically driven nonholonomic mobile robot via backstepping and fuzzy approach. IEEE Transactions on Control Systems Technology **17**(4), 803–815 (2009)
10. Jia, S., Shan, J.: Finite-time trajectory tracking control of space manipulator under actuator saturation. IEEE Transactions on Industrial Electronics (2019)
11. Ma, O., Martin, E.: Extending the capability of attitude control systems to assist satellite docking missions. In: Proceedings CCToMM Symposium on Mechanisms, Machines, and Mechatronics (2001)
12. Nguyen-Huynh, T., Sharf, I.: Adaptive reactionless motion and parameter identification in postcapture of space debris. Journal of Guidance Control and Dynamics. **36**(2), 404–414 (2013)
13. Oki, T., Abiko, S., Nakanishi, H., Yoshida, K.: Time-optimal detumbling maneuver along an arbitrary arm motion during the capture of a target satellite. In: Prco. of IEEE/RSJ International Conference on Intell. Robots and Systems, pp. 625–630 (2011)
14. Papadopoulos, E.: On the dynamics and control of space manipulators. Ph.D. thesis, Dept. of Mech. Eng., MIT, Cambridge (1990)
15. Polycarpou, M., Ioannou, P.: A robust adaptive nonlinear control design. Automatica **32**(3), 423–427 (1996)
16. de Ruiter, A.: Spacecraft attitude tracking with guaranteed performance bounds. Journal of Guidance, Control, and Dynamics **36**(4), 1214–1221 (2013)
17. Wang, M., Luo, J., Yuan, J., Walter, U.: Detumbling control for kinematically redundant space manipulator post-grasping a rotational satellite. Acta Astronautica **141**, 98–109 (2017)
18. Wang, M., Luo, J., Yuan, J., Walter, U.: An integrated control scheme for space robot after capturing non-cooperative target. Acta Astronautica **147**, 350–363 (2018)
19. Xavier, C., Gilber, J.: Postcapture dynamics of a spacecraft-manipulator-payload system. Journal of Guidance Control and Dynamics **23**(1), 95–100 (2000)
20. Yoshida, K.: The spacedyn: a matlab toolbox for space and mobile robots. In: Proc. of IEEE/RSJ International Conference on Intell. Robots and Systems, pp. 1633–1638. Kyongju, South Korea (1999)
21. Yoshida, Y., Dimitrov, D.: On the capture of tumbling satellite by a space robot. In: Proc. of IEEE/RSJ International Conference on Intell. Robots and Systems, pp. 4127–4132. Beijing (2006)
22. Zhang, B., Liang, B., Wang, Z., Mi, Y., Zhang, Y., Chen, Z.: Coordinated stabilization for space robot after capturing a non-cooperative target with large inertia. Acta Astronautica **134**, 75–84 (2017)
23. Zou, A., Kumar, K., de Ruiter, A.: Robust attitude tracking control of spacecraft under control input magnitude and rate saturations. International Journal of Robust and Nonlinear Control **26**(4), 799–815 (2016)